Taylor & Francis
Taylor & Francis Group

Check for updates

RESEARCH PAPER

# MiR-3138 deteriorates the insulin resistance of HUVECs via KSR2/AMPK/GLUT4 signaling pathway

Yan Chen[a,b,d], Da Lin[c], Changxuan Shi[c], Liang Guo[c], Linhua Liu[b], Lin Chen[b], Ting Li[b], Ying Liu[b], Chengchao Zheng[d], Xintong Chi[d], Chun Meng[c], and Yaoming Xue[a]

[a]Department of Endocrinology and Metabolism, Nanfang Hospital, Southern Medical University, Guangzhou, Guangdong Province, China; [b]Department of Internal Medicine, South Branch of Fujian Provincial Hospital, Fuzhou, Fujian Province, China; [c]Institute of Pharmaceutical Biotechnology and Engineering, College of Biological Science and Biotechnology, Fuzhou University, Fuzhou, Fujian Province, China; [d]Provincial Clinic Medical College, Fujian Medical University, Fuzhou, Fujian Province, China

## ABSTRACT

Insulin resistance (IR) is a complex pathological condition resulting from the dysregulation of cellular response to insulin hormone in insulin-dependent cells and is recognized as a pathogenic hallmark and strong risk factor for metabolic syndrome. The present study aims to elucidate the molecular mechanism of the pathogenesis of IR. Here, we used human umbilical vein endothelial cells (HUVECs) to establish the IR cell model induced by $1 \times 10^{-6}$ mmol/L insulin. After 48 h, reactive oxygen species (ROS) and glucose consumption were measured by DCFH-DA and GOD-POD methods, respectively. The results of Microarray analysis demonstrated that there were 10 differentially expressed miRNAs (DEMs) selected based on Fold change (FC) and P value in the IR cell model compared with HUVECs. The enriched gene ontology (GO) terms analysis showed that the target genes of these 10 DEMs were significantly enriched in biological process, cellular component and molecular function, and the significantly enriched Kyoto Encyclopedia of Genes or Genomes (KEGG) pathways mainly include AMPK signaling pathway and PI3K signaling pathway. Amongst all, the expression level of miR-3138 was highest in the IR cell model evaluated by qRT-PCR. Through Targetscan, KSR2 mRNA was predicted as a target of miR-3138. And mRNA and protein expression levels of miR-3138, KSR2, GLUT4, AMPK, PI3K, Akt were examined using qRT-PCR and Western blotting, respectively. The interaction between miR-3138 and KSR2 was evaluated by dual-luciferase reporter assay. Our results showed that miR-3138 significantly deteriorated the IR of HUVECs via KSR2/AMPK/GLUT4 signaling pathway.

## Introduction

IR is characterized by decreased response of cells to insulin stimulation. IR induces metabolic syndrome in livers, muscles and adipose tissues [1], such as hyperglycemia, hyperuricemia, hypertension, elevated inflammatory markers, endothelial dysfunction, and prothrombotic state [2]. Moreover, IR impairs glucose disposal and increases beta-cell insulin secretion and hyperinsulinemia. Recent studies showed that IR is recognized as a pathogenic hallmark of reduced glucose consumption and a risk factor for diabetes and related cardiovascular diseases [3,4]. However, the key molecules involved in IR remain unknown.

Multiple factors are involved in the specific pathogenesis of IR. For example, high-glucose level impairs insulin signaling, and is closely associated with IR [5]; an elevated level of reactive oxygen species (ROS) has been observed in cell and eventually contributes to IR [6]. In addition, miRNAs contribute to islet cell injury, apoptosis and IR-related cell abnormalities by affecting the occurrence, development and complications of diseases [7–12]. There is also a recent research showing that Kinase suppressor of ras 2 (KSR2) plays an important role in maintaining energy balance and reducing insulin sensitivity via activation of the energy sensor AMP-activated protein kinase (AMPK) [13]. KSR2 interacting with AMPK may play significant roles in high insulin level and impaired glucose tolerance [14–17]. Meanwhile, abnormal expression of KSR2 enhances AMPK phosphorylation and signaling in a cell-autonomous manner [18]. It was reported

that glucose transporter isoform 4 (GLUT4) acting as an insulin-responsive glucose transporter is entirely dependent on insulin and could translocate into cell membrane and facilitate glucose to enter cells [19]. Recent research has shown that GLUT4 sensitively responses to insulin in endothelium cells [20–22] and insulin could promote the expression and translocation of GLUT4 in endothelium [23].

Given the indispensable significance of IR in clinical practice, it is important to elucidate the molecular mechanism of IR. In this study, we used HUVECs to establish the IR cell model. Subsequently, a bioinformatics study was carried out based on the microarray profiling. In order to explore the potential molecular function of DEMs between IR cell model and HUVECs, GO analysis and KEGG pathway analysis were performed. The DEMs were verified by qRT-PCR and miR-3138 showed high expression level in IR cell model. Finally, we found that miR-3138 directly interacting with KSR2 could regulate the expression of GLUT4 and the phosphorylation of AMPK in IR cell model which were validated by cell experiments in vitro. Our findings provide mechanistic insights into the occurrence and a novel strategy of IR.

## Methods

### Materials and agents

PCR primers, DNA fragments, siRNA fragments, DNA modification enzymes, DNA endonuclease, RNA extraction reagent, and reverse transcription reagent were purchased from Invitrogen (Thermo Scientific). Fetal bovine serum and cell culture medium were purchased from Gibico (Thermo Scientific). Plasmid DNA and purification kits were purchased from Biyuntian, and monoclonal antibodies were purchased from Abcam (San Francisco). Relative antibodies were purchased from Cell Signaling Technology (CST, Danvers, MA). Human umbilical vein endothelial cells (HUVECs) were purchased from the American Culture Collection (VA Manassas).

### Construction of the IR cell model and cell groups

HUVECs were cultured in Dulbecco's Modified Eagle's medium (DMEM) (Gibco, Thermo Fisher Scientific) supplemented with penicillin (100 U/ml), streptomycin (100 μg/ml) and 10% fetal bovine serum at 37°C with 5% $CO_2$. We determined 48 h as the optimal time for insulin stimulation in consideration of cell passage time. HUVECs were grown in normal medium with 10 mmol/L glucose for 24 h as the negative control (NC) group, while high-glucose-treated cells were grown in medium with 35 mmol/L glucose for 24 h to lead to the glucose metabolism disorder [24,25]. When the cells were grown to reach 90% confluence, the medium was replaced with DMEM containing various concentrations of insulin ($1 \times 10^{-7}$, $1 \times 10^{-6}$ and $1 \times 10^{-5}$ mmol/L) for 24 h in order to establish IR cell model.

Except the experiments of efficiency of KSR2 silencing and dual-luciferase assays, HUVECs were grouped as follows. HUVECs were divided into five groups: HUVECs with no intervention (negative control, NC), miR-3138 transfection (NC+miR-3138 overexpression), miR-Con transfection (NC+miR-Con overexpression), KSR2 siRNA1 transfection (NC+KSR2 silencing), KSR2-Con siRNA transfection (NC+ KSR2-Con silencing). IR cell models were divided into six groups: IR cell models with no intervention (IR), miR-3138 transfection (IR+miR-3138 overexpression), miR-Con transfection (IR+miR-Con overexpression), miR-Con inhibitor transfection (IR+ miR-Con inhibition), both transfection of miR-3138 inhibitor and KSR2 siRNA1 (IR+miR-3138 inhibition+KSR2 silencing), both transfection of miR-3138 inhibitor and KSR2-Con siRNA (IR+miR-3138 inhibition+KSR2-Con silencing). All the sequences designed for experiments including miR-3138, miR-3138 inhibitor, miR-Con, miR-Con inhibitor, KSR2 siRNA1, KSR2-Con siRNA were shown inSupporting Table S1.

### Efficiency of KSR2 silencing

The KSR2 siRNA targets were designed using short hairpin. The KSR2 nucleotide sequence was synthesized by Shanghai Sangon Biotechnology. Two specific siRNAs of targeting KSR2 (KSR2 siRNA-1 and KSR2 siRNA-2) and another siRNA (KSR2-Con siRNA) (Shanghai Sangon Biotech) as control were designed using online siRNA design

tool (http://www.mwg-biotech.com). The sequence of KSR2 siRNA2 was shown in supporting table S1. For the KSR2 silencing experiment, HUVECs were divided into four groups: HUVECs with no intervention (NC), KSR2 siRNA1 transfection (KSR2 silencing-1), KSR2 siRNA2 transfection (KSR2 silencing-2), KSR2-Con siRNA transfection (KSR2-Con silencing). siRNAs at a concentration of 20 pmol/μl were stored at −20 °C. HUVECs ($5.0 \times 10^5$/well) were seeded onto a 12-well culture plate. Solution A was prepared by adding 2 μl of lipofectamine reagent (Gibco, Thermo Fisher Scientific) into 200 μl of serum-free DMEM. Solution B was prepared by adding 4 μl of siRNA (siRNA-1 or siRNA-2) into 200 μl of serum-free DMEM (Gibco, Thermo Fisher Scientific). The transfection solution was prepared by slowly adding solution B to solution A. The mixture was agitated and then incubated at room temperature for 20 min, and then added to each well. The cells were cultured with the transfection solution in an incubator containing 5% $CO_2$ at 37 °C for 5 to 6 h. The supernatant was then replaced by culture medium and the cells were cultured at 37 °C for 48 h.

## RNA extraction, miRNA labeling and array hybridization

Total RNA was isolated from the cells using Trizol reagent (Invitrogen, Carlsbad) and purified with a miRNeasy mini kit (Qiagen, Dusseldorf). RNA quality control was performed to ensure the high quality of RNA samples for microarray analysis, and the purity was examined using spectrophotometry, with the acceptable threshold defined as OD260/OD280 > 2.0 and OD260/OD230 > 1.8. Electrophoresis was used to analyze RNA integrity, with the acceptable threshold defined as 28S/18S >2.

After quality control, the miRCURY™ Hy3™/Hy5™ Power labeling kit (Exiqon,

Vedbaek was used according to the manufacturer's guideline for miRNA labeling. Then, the Hy3™-labeled samples were hybridized on the miRCURY$^{TM}$ LNA Array (v.19.0) (Exiqon) according to array manual. Finally, the slides were scanned using the Axon Gene Pix 4000B microarray scanner (Axon Instruments, Foster).

## Microarray and bioinformatics analyses of miRNAs

Microarray experiments were performed to analyze the DEMs between IR groups and NC groups. The cells from the NC groups and the IR groups (insulin intervention at $1x10^{-6}$mmol/L concentration) were separately collected for analysis. Three parallel repeats were set in each group. The array images captured were analyzed using Feature Extraction software 10.7 (Agilent Technologies) with default settings. Raw data were normalized by the Quantile algorithm in Gene Spring Software 12.6 (Agilent Technologies). The 10 DEMs were selected based on both FC and P value. Potential target genes of the DEMs were predicted using Targetscan (http://targetscan.org/), miRbase (http://mirdb.org/miRDB/) and miRanda (http://www.miranda.org/). The target genes of the DEMs were subjected to gene ontology (GO) analysis (http://geneontology.org/) and Kyoto encyclopedia of genes and genomes (KEGG) pathway analysis (https://www.kegg.jp/). P value less than 0.05 was considered to be statistically significant.

## Quantitative reverse transcription-polymerase chain reaction (qRT-PCR)

The 10 DEMs determined through the array data analysis were further validated by qRT-PCR. qRT-PCR was performed using SYBR-Green (Invitrogen) according to the manufacturer's instructions in a Rotor-Gene 3000 Real-time PCR instrument (Corbett Research, Brisbane). U6 served as an internal control. The relative expression of each miRNA was calculated using the comparative Ct ($2^{-\Delta\Delta Ct}$) method, and the results were examined by t-test. The primers used in reverse transcription and PCR are listed in Supporting Table S1.

## Transfection of miRNA

The HUVECs were separately transfected with 0.1 nmol miR-3138 (Ribobio), miR-Con, miR-3138 inhibitor and miR-Con inhibitor in the presence of Lipofectamine 2000 (Invitrogen). After 48 h incubation at 37°C, the cells in the 24-well

plate were starved in Krebs-Ringer bicarbonate HEPES medium for 24 h.

## Dual-luciferase assays

The cells were seeded into 96-well plates, grown overnight, and then incubated in serum-free DMEM for 6 h before cell transfection. The wild-type 3'UTR sequence of KSR2 (WT-KSR2), corresponding mutant with mutations in the predicted binding sites (MT-KSR2), and the irrelevant gene (KSR2-Con) were all synthesized and ligated into the pGL6 Dual-Luciferase miRNA Target Expression Vector (Promega, Madison, WI) and named as pGL6-WT-KSR2, pGL6-MT-KSR2 and pGL6-KSR2-Con, respectively. Then, the cells were transfected with pGL6-WT-KSR2 + miR-3138, pGL6-WT-KSR2+ miR-Con, pGL 6-MT-KSR2+ miR-3138, pGL6-MT-KSR2+ miR-Con, pGL6-KSR2-Con+miR-3138, pGL6-KSR2-Con +miR-Con. After transfecting for 48 h, Dual Luciferase Assay (Promega) was used to test the activities of Firefly and Renilla luciferase consecutively.

## Glucose consumption assay

HUVECs were cultured in 96-well culture plates. Cell supernatants were collected after cell treatment for 24 h. The glucose oxidase and peroxidase (GOD-POD) method was used to determine the glucose concentration after various treatments HUVECs for 24 h. The glucose consumption was calculated by subtracting the glucose concentration of each well from the glucose concentration of the blank wells.

## Measurement of intracellular ROS

The intracellular ROS generation was measured by oxidative-sensitive fluorescent probe 2',7'-dichlorofluorescindiacetate (DCFH-DA). Cell supernatants were collected after cell treatment for 24 h. The HUVECs were incubated with 10 μmol DCFH-DA in culture medium at 37°C for 30 min. The cells were washed with phosphate-buffered saline (PBS) to remove the additional DCFH-DA. Finally, fluorescence was detected at 485 nm for excitation and at 530 nm for emission using a microplate reader (Perkin Elmer Victor 2) [26].

## Western blotting

The cells were lysed using RIPA lysis buffer. Total proteins in the lysate were obtained by centrifugation. The obtained proteins were separated on SDS-PAGE (sodium dodecyl sulfate-polyacrylamide) gel and then transferred to PVDF (polyvinylidene fluoride) membranes. Membranes were blocked with 5% nonfat milk. After blotting, membranes were incubated with primary antibodies against studied proteins and actin (sc-1615, Santa Cruz). The reaction was detected with a Western blotting detection system (Thermo Scientific, Rockville).

## Statistical analysis

All the experiments were performed in triplicate. The data were shown as mean ± SD. Significant differences between different sets of data were analyzed by two-tailed Student's $t$-test or one-way ANOVA using the SPSS 12.0 software. $P < 0.05$ was defined as statistically significant.

## Results

### Establishment of IR cell model

In the present study, three different concentrations ($1 \times 10^{-5}$ mmol/L, $1 \times 10^{-6}$ mmol/L and $1 \times 10^{-7}$ mmol/L) of insulin were used for HUVECs glucose consumption analysis, while the insulin concentration of $1 \times 10^{-7}$ mmol/L led to accidental cell death similarly to literature report. Compared with the NC group, the glucose consumption of the HUVECs group with $1 \times 10^{-6}$ mmol/L insulin was the lowest (Figure 1, $P < 0.001$). Thus, we established the IR cell model cultured in DMEM and induced by $1 \times 10^{-6}$ mmol/L insulin for 48 h which was used for further experiments.

### Efficiency of KSR2 silencing

To investigate the role of KSR2 in HUVECs, KSR2 was silenced. The mRNA and protein expression of KSR2 after various silencing treatments were detected by qRT-PCR and Western blotting, to evaluate the efficiency of silencing. Compared with the NC group, both the mRNA and protein expressions of KSR2 after siRNA1 silencing and
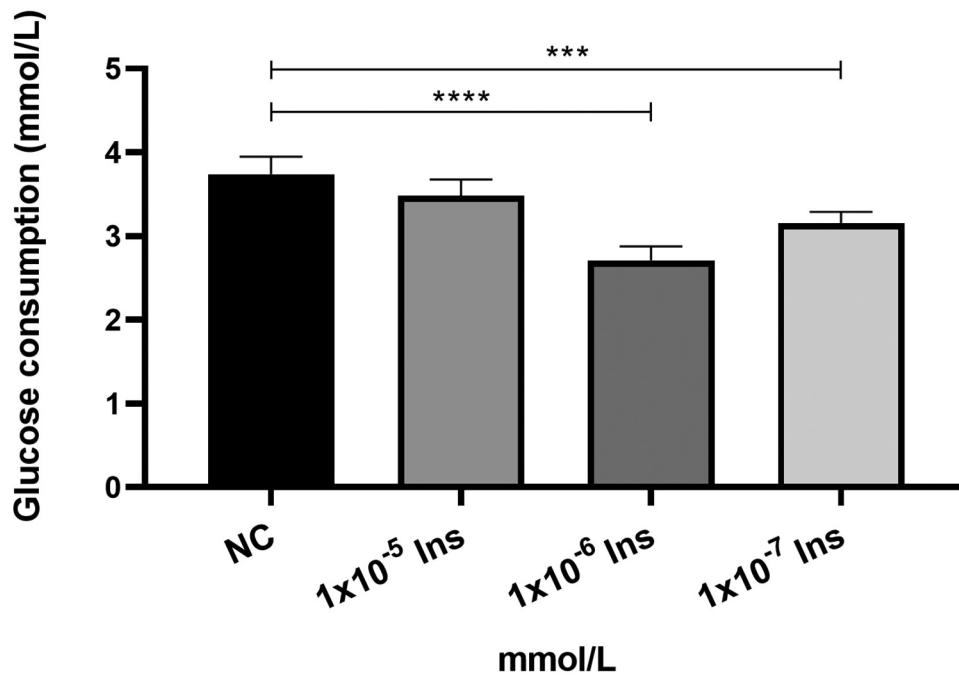
**Figure 1.** Glucose consumption after treatments HUVECs with various insulin concentrations. Amongst all, the glucose consumption in the $1 \times 10^{-6}$ mmol/L insulin group was the lowest. The values were expressed as mean $\pm$ S.D. at three independent experiments performed in triplicate. ***P < 0.005, ****P < 0.001, vs. NC.

siRNA2 silencing were significantly reduced (Figure 2a, P < 0.001 and P < 0.01, respectively; Figure 2b-2c, P < 0.01 and P < 0.05, respectively). In addition, we found that the mRNA and protein expressions of KSR2 after siRNA1 silencing were reduced to about 1/5 and 1/3 of those in the NC group (Figure 2a-c). Thus, siRNA1 was used to silence KSR2 for further experiments.

## DEMs identification in IR cell model and GO and KEGG pathway enrichment analysis

After being compared with NC groups, the results of microarray profile showed that there were a total of 827 miRNAs with 4 up-regulated miRNAs and 6 down-regulated miRNAs in the IR groups based on the principle of $|\log_2 FC(IR/NC)| \geq 1.0$ and P value $\leq 0.01$ (Figure 3a-b). Then, the 10 DEMs were selected to perform bioin formatics analysis, including 4 up-regulated miR NAs (miR-381-5p, miR-3138, miR-382-3p and miR-671-5p) and 6 down-regulated miRNAs (miR-4521, miR-1267, miR-372-5p, miR-2681-3p, miR-892a and miR-193-5p). The up-regulated

**Table 1.** Fold changes (FCs) and P values of differentially expressed miRNAs (DEMs).

| miRNAs down-regulated in IR group vs. NC group | | | miRNAs up-regulated in IR group vs. NC group | | |
|---|---|---|---|---|---|
| Unique ID | FC | P value | Unique ID | FC | P value |
| hsa-miR-1267 | 0.173 | 0.006 | hsa-miR-381-5p | 4.012 | 0.005 |
| hsa-miR-193b-5p | 0.160 | 0.007 | hsa-miR-671-5p | 2.017 | 0.005 |
| hsa-miR-2681-3p | 0.155 | 0.003 | hsa-miR-3138 | 3.811 | 0.007 |
| hsa-miR-372-5p | 0.247 | 0.009 | hsa-miR-382-3p | 3.362 | 0.001 |
| hsa-miR-4521 | 0.027 | 0.008 | | | |
| hsa-miR-892a | 0.051 | 0.009 | | | |

Captions: The fold change (FC) (IR vs.NC) and P values of DEMs were shown in Table 1. There were 6 down-regulated miRNAs and 4 up-regulated miRNAs based on FC and P values.

miRNAs were selected based on the principle of $\log_2 FC(IR/NC) \geq 1.0$ and P value $\leq 0.01$, and, the down-regulated miRNAs were selected based on the principle of $\log_2 FC(IR/NC) \leq -1.0$ and P value $\leq 0.01$ (Figure 3b, Table 1).

These 10 DEMs were used for target gene prediction by Targetscan (http://targetscan.org/), miR base (http://mirdb.org/miRDB/) and miRanda (http://www.miranda.org/). The enriched GO terms and KEGG pathways analysis were identified for the predicted target genes which were
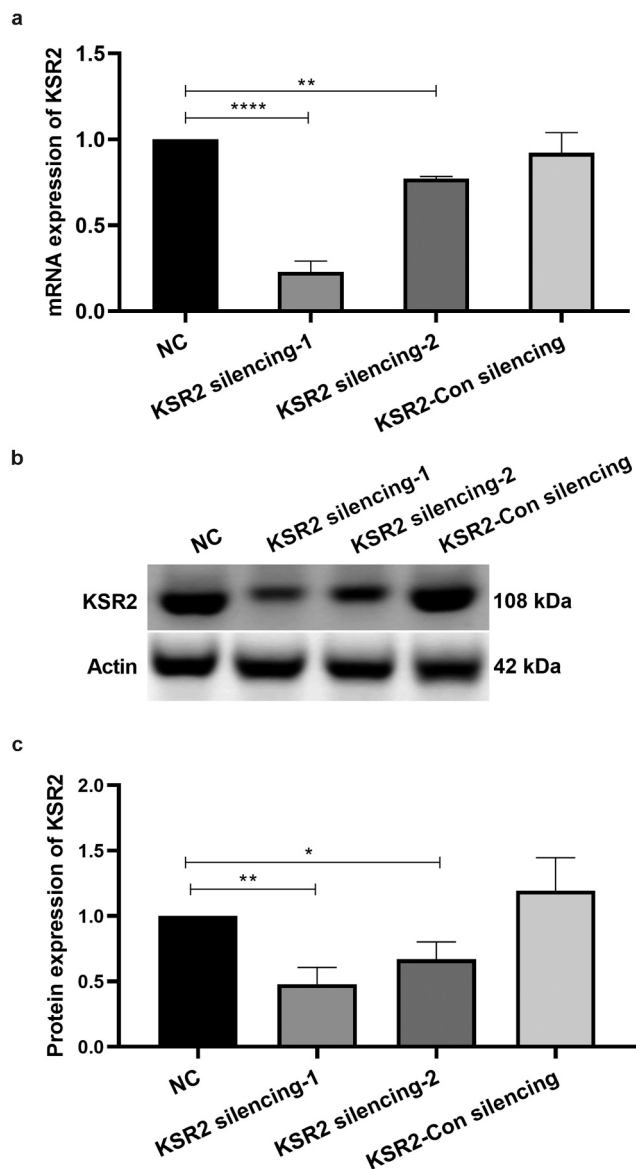
**Figure 2.** Efficiency of KSR2 silencing. (a)The mRNA expression of KSR2 after various silencing treatments was detected by qRT-PCR. And the values were measured at three independent experiments in triplicate. The mRNA expression of KSR2 in NC group was used for normalization control. **$P < 0.01$, ****$P < 0.001$ vs. NC. (b) The protein expression of KSR2 after various silencing treatment was detected by Western blotting. (c) The protein expression of KSR2 after various silencing treatment was detected by Western blotting. The values were measured at three independent experiments in triplicate. The densitometric analysis was performed using ImageJ software and normalizing to actin. The protein expression of KSR2 in NC group was used for normalization control. *$P < 0.05$, **$P < 0.01$ vs. NC.

performed to explore the molecular functions and analyze their related signaling pathways. According to the P-values, the top 10 enriched terms were shown in Figure 3c-e. The predicted target genes were significantly enriched in biological process (BP, Figure 3c, $P < 0.05$), cellular component (CC, Figure 3d, $P < 0.05$), and molecular function (MF, Figure 3e, $P < 0.05$). Besides, the significantly enriched pathways were illustrated in Figure 3f (p<0.05). The significantly enriched pathways mainly included AMPK signaling pathway (Figure 3g, $P = 0.03$) and the PI3K/Akt pathway (Figure 3h, $P = 0.02$).

## Evaluation of differentially expressed miRNAs in IR cell model

The 10 DEMs from bioinformatics results were evaluated by qRT-PCR. As is illustrated in Figure 4a, the IR groups exhibited a significantly higher expression levels of miR-381-5p and miR-3138 than the NC groups (2.60 times and 6.31 times vs. NC, $P < 0.001$, respectively). Moreover, the expression level of miR-3138 in IR group was highest than other groups (Figure 4a, $P < 0.001$). Although the expressions of miR-382-3p, miR-671-5p, miR-4521, miR-892a and miR-2681-3p in the IR groups were also increased compared to the NC groups, no statistical differences were seen in these data (Figure 4a). In addition, no statistical differences were seen in the reduced expression of miR-1267, miR-372-5p and miR-193-5p in comparison with the NC groups (Figure 4a).

Further, we carried out the rescue experiment to verify the miR-3138 expression, under IR condition. As shown in Figure 4b, miR-3138 expression was increased in the IR group compared with the NC group (Figure 4b, $P < 0.001$). And, under the IR condition, miR-3138 expression was decreased after inhibition of miR-3138 which verified the inhibition efficiency of miR-3138 inhibitor (Figure 4b, $P < 0.001$). The effect of miR-3138 inhibition on the mRNA expression of miR-3138 could explain that there was no significant difference in mRNA expression of miR-3138 between the IR+miR-3138 inhibition+ KSR2-Con silencing group and the IR+miR-3138 inhibition+KSR2 silencing group (Figure 4b). Thus, we selected miR-3138 as the promising gene to interpret the molecular mechanism of IR.
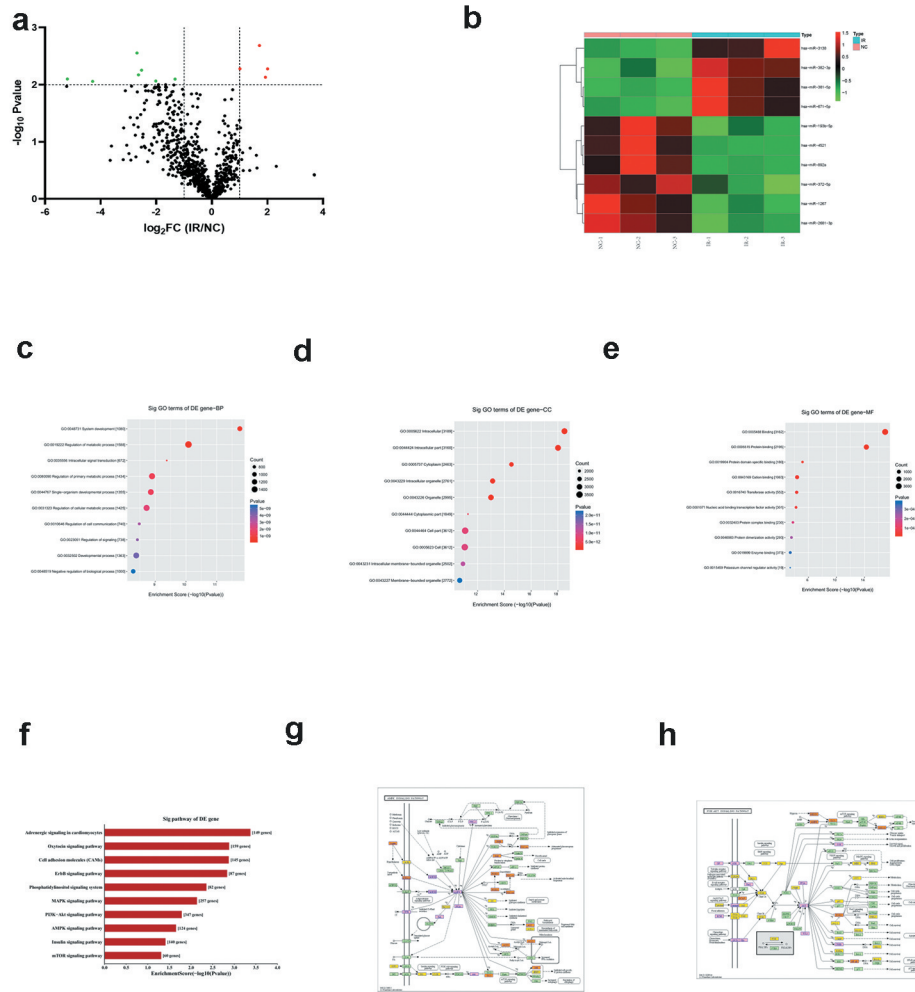
**Figure 3.** miRNA expression profile of IR groups vs. NC groups and GO and KEGG pathway analysis. (a)Analyzed miRNAs plotted in a volcano plot. A red dot represents a miRNA with $\log_2$ FC(IR/NC) $\geq$ 1.0 and P $\leq$ 0.01. A green dot represents a miRNA with $\log_2$ FC (IR/NC) $\leq$ −1.0 and P $\leq$ 0.01. (b) Heat map for DEMs between IR groups and NCs with |$\log_2$ FC(IR/NC) | $\geq$ 1.0 and P $\leq$ 0.01. Each row represents a miRNA and differential expression levels are illustrated by the pseudocolor. Red indicates high expression level, green indicates low expression level, and black indicates mean expression level. (c) The enriched GO terms for biological process (BP). The dot plot shows the 10 most enriched score values of the significant enrichment terms (P < 0.05). (d) The enriched GO terms for cellular component (CC). The dot plot shows the 10 most enriched score values of the significant enrichment terms (P < 0.05). (e) The enriched GO terms for molecular function (MF). The dot plot shows the 10 most enriched score values of the significant enrichment terms (P < 0.05). (f) KEGG pathways significantly enriched by AMPK signaling pathway and PI3K/Akt pathway. The histogram shows the 10 most enriched score values of the significantly enriched pathways (P < 0.05). (g) The AMPK signaling pathway (P = 0.03). (h) The PI3K/Akt pathway (P = 0.02).

## Effects of miR-3138 and KSR2 on IR

Compared with the NC group, glucose consumption was reduced in the IR group (Figure 5a, P < 0.001). And, KSR2 silencing and miR-3138 overexpression had the same effect (Figure 5c, P < 0.001, respectively). In addition, ROS content in the IR group was markedly higher than that in the NC group (Figure 5b, P < 0.005). Furthermore, miR-3138 overexpression had the same effect, under IR condition (Figure 5b, P < 0.001). The transfection of miR-Con into IR group had no significant effects on the glucose consumption and ROS content compared with the IR group which showed suitable control of the experiments (Figure 5a-b). Therefore, the enhancement effect of miR-3138 and the alleviation effect of KSR2 on IR were verified preliminary.
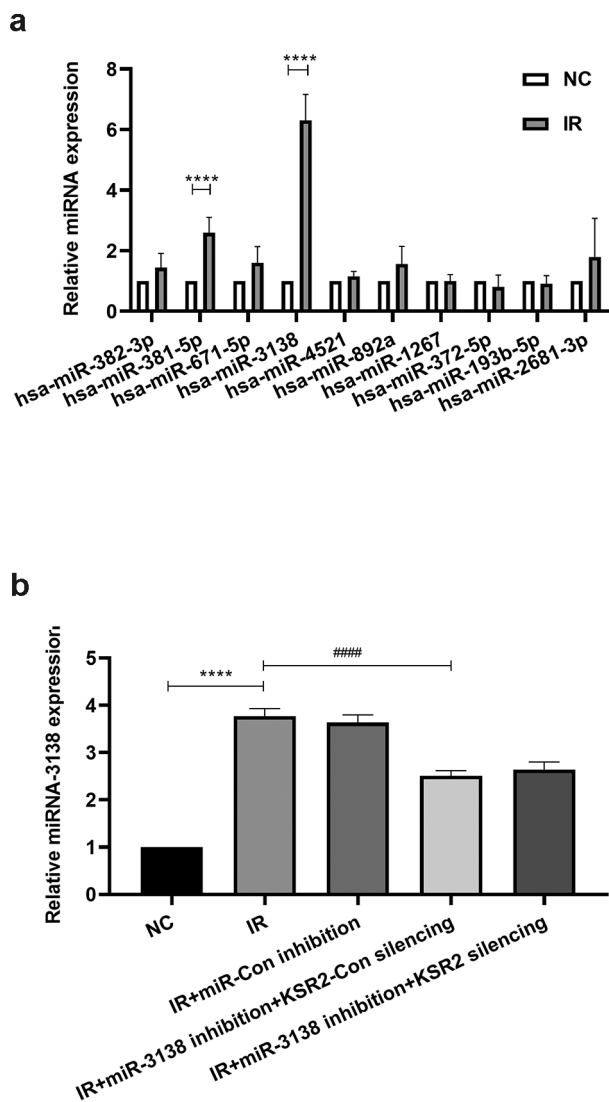
**a**



**b**



**Figure 4.** (a) Validation of 10 DEMs obtained from the microarray profile by qRT-PCR. The relative expressions of miRNAs were calculated from three independent experiments after normalization with the expressions in NC groups. ****$P < 0.001$ vs. NC. (b) Under IR condition, the relative miR-3138 expression after various treatments HUVECs underwent miR-Con inhibition, miR-3138 inhibition + KSR2-Con silencing or miR-3138 inhibition + KSR2 silencing. The relative expression of miR-3138 was calculated from three independent experiments after normalization with the expression in NC group. ****$P < 0.001$ vs. NC; ####$P < 0.001$ vs. IR.

We also performed rescue experiments to get further evidence about effects of miR-3138 and KSR2 on IR. Consistent with the previous results (Figure 5a-b), glucose consumption and ROS content in the IR groups were decreased and increased compared with the NC groups, respectively (Figure 5d-e, $P < 0.001$, respectively). And, under IR condition, glucose consumption was increased

after miR-3138 inhibition compared with the IR group, but reduced when miR-3138 inhibition and KSR2 silencing compared with the IR+miR-3138 inhibition+KSR2-Con silencing group (Figure 5d, $P < 0.001$, respectively). Inhibition of miR-3138 triggered a decrease in ROS content compared with the IR group, whereas the reduction was partly inverted by KSR2 silencing (Figure 5e, $P < 0.001$, respectively). Thus, our results confirmed the effects of miR-3138 and KSR2 on enhancing and alleviating the IR of HUVECs, respectively.

## MiR-3138 directly targets KSR2

Bioinformatic analysis by Targetscan showed a seeding area of miRNA-3138 in the 3'-UTR of the KSR2 gene: 5'-GUCCAC-3' (Figure 6a). To validate whether KSR2 was a target of the miR-3138 in IR cell model, the wild-type 3'UTR sequence of KSR2 (WT-KSR2) and mutant with mutations in the predicted binding sites (MT-KSR2) also with the irrelevant gene (KSR2-Con) were all synthesized and ligated into the pGL6 Dual-Luciferase miRNA Target Expression Vector. The luciferase activities of Firefly and Renilla were measured, respectively, and the ratio of Firefly/Renilla was determined. Our results showed that co-transfection of miRNA-3138 significantly inhibited the activity of firefly luciferase reporter with wild-type 3'-UTR of KSR2, but not of those with the mutant 3'-UTR and KSR2-Con (Figure 6b, $P < 0.001$, respectively).

In order to further determine the effect of miR-3138 on suppressing KSR2 expression, miR-3138 was overexpressed or inhibited in HUVECs which were then subjected to determine the protein expressions of KSR2 detected by Western blotting analysis. Compared with the NC group, we found that KSR2 expression was significantly reduced in the IR group and in the NC+miR-3138 overexpression group (Figure 6c-d, $P < 0.001$, respectively). The NC+miR-Con overexpression group had no significant effects on the protein expression of KSR2 compared with the NC group which showed suitable control of the experiments. Therefore, we speculated that both IR and miR-3138 overexpression could decrease the expression of KSR2.
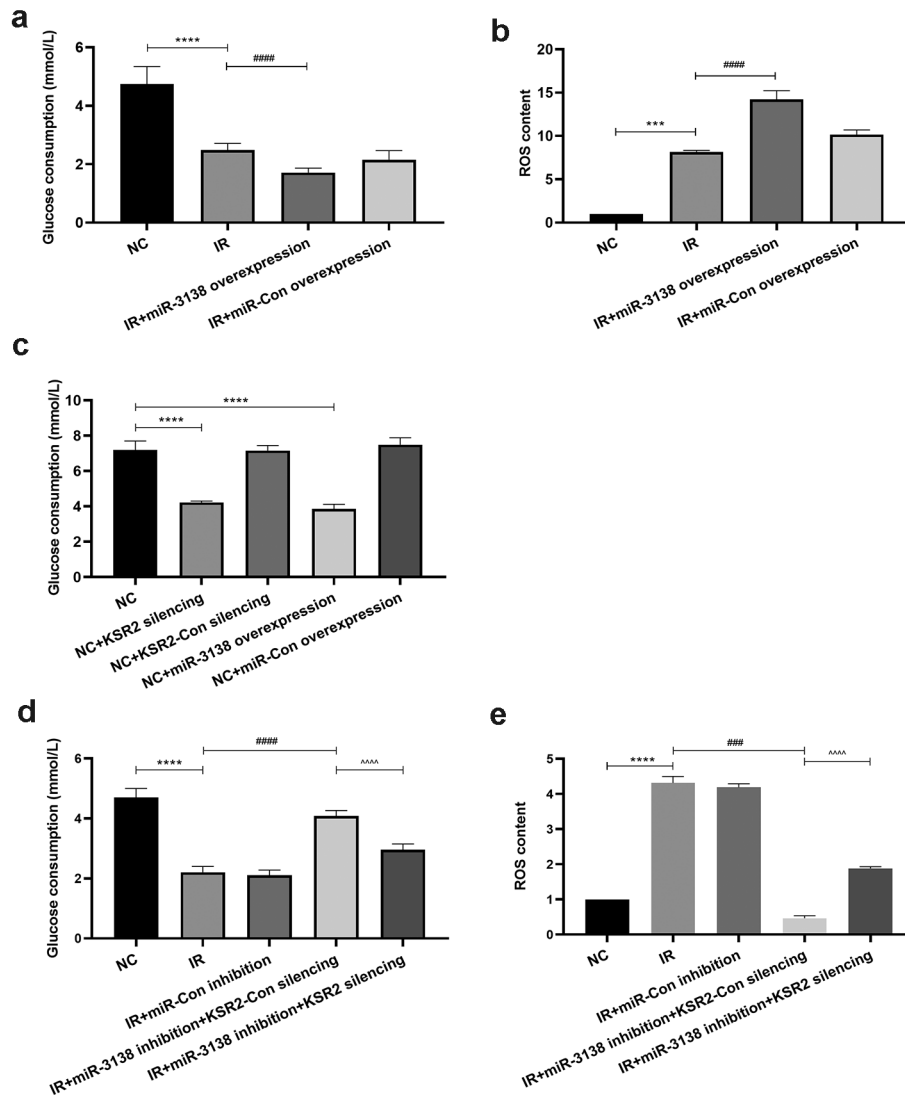
**Figure 5.** Effects of miR-3138 and KSR2 on IR. (a) Under IR condition, the glucose consumption after various treatments HUVECs underwent miR-3138 overexpression or miR-Con overexpression. The scale bars represent the mean ± S.D. of at least three independent experiments performed in triplicate. ****$P < 0.001$ vs. NC, ####$P < 0.001$ vs. IR. (b) Under IR condition, the ROS content after various treatments HUVECs underwent miR-3138 overexpression or miR-Con overexpression. The ROS content was calculated from three independent experiments after normalization with the value in NC group. ***$P < 0.005$ vs. NC, ####$P < 0.001$ vs. IR. (c) The glucose consumption after various treatments HUVECs underwent KSR2 silencing, KSR2-Con silencing, miR-3138 overexpression or miR-Con overexpression. The scale bars represent the mean ± S.D. of at least three independent experiments performed in triplicate. ****$P < 0.001$ vs. NC. (d) Under IR condition, the glucose consumption after various treatments HUVECs underwent miR-Con inhibition, miR-3138 inhibition + KSR2-Con silencing or miR-3138 inhibition + KSR2 silencing. The scale bars represent the mean ± S.D. of at least three independent experiments performed in triplicate. ****$P < 0.001$ vs. NC; ####$P < 0.001$ vs. IR. ^^^^$P < 0.001$ vs. IR+ miR-3138 inhibition+KSR2-Con silencing. (e) Under IR condition, the ROS content after various treatments HUVECs underwent miR-Con inhibition, miR-3138 inhibition + KSR2-Con silencing or miR-3138 inhibition + KSR2 silencing. The ROS content was calculated from three independent experiments after normalization with the value in NC group. ****$P < 0.001$ vs. NC; ####$P < 0.001$ vs. IR; ^^^^$P < 0.001$ vs. IR+ miR-3138 inhibition + KSR2-Con silencing.

Further, we carried out rescue experiments to explore the effect of miR-3138 on mRNA and protein expressions of KSR2, under IR condition (Figure 6e-g). Consistent with the results shown in Figure 6d, the mRNA and protein expressions of KSR2 were significantly reduced in the IR groups compared with the NC group (Figure 6e-g, $P < 0.001$, $P < 0.005$, respectively). And, under IR condition, the mRNA expression of KSR2 was increased to 3.53 times after miR-3138 inhibition compared with the IR group, but reduced significantly when miR-3138 inhibition and KSR2 silencing
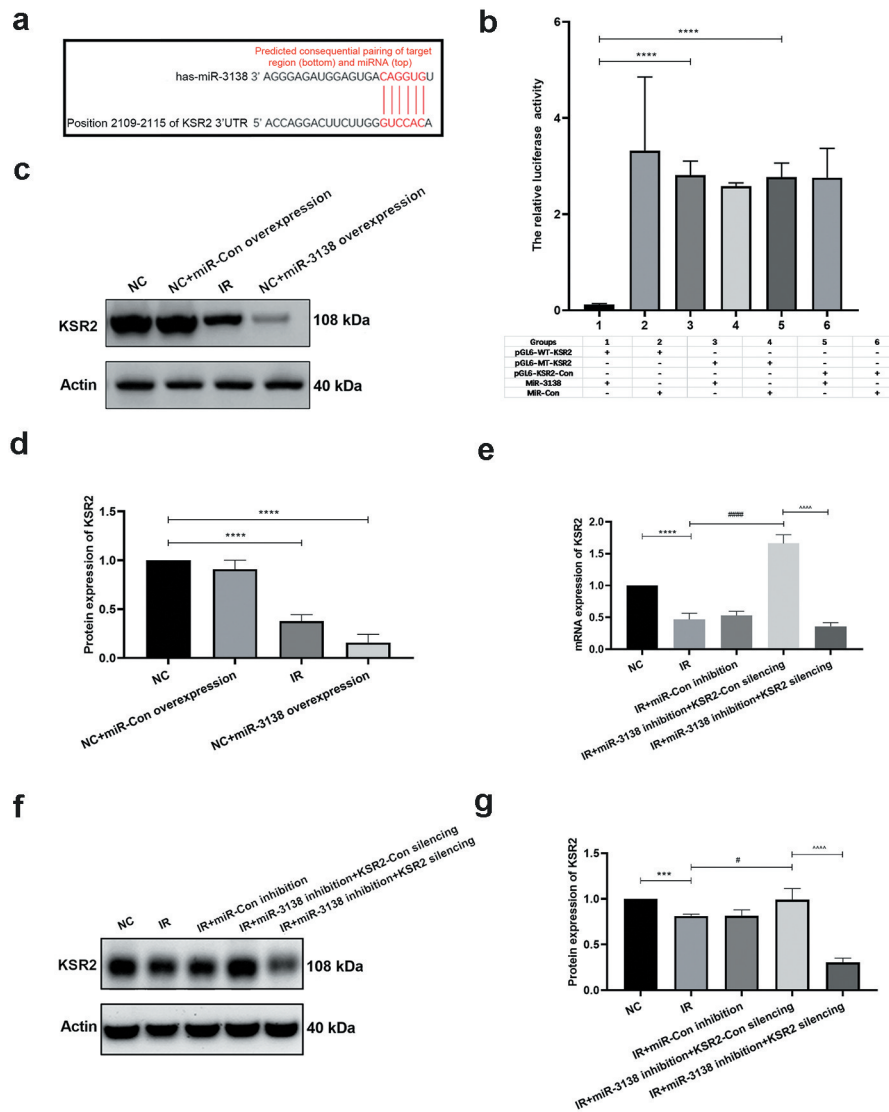
**Figure 6.** miR-3138 directly targets KSR2. (a)Representation of KSR2 and the relative position of the predicted miR-3138-binding sites (http://www.targetscan.org). (b) Dual-luciferase reporter assay of HUVECs. HUVECs were transfected with pGL6-WT-KSR2 luciferase vector, pGL6-MT-KSR2 luciferase vector, pGL6-KSR2-Con vector, miR-3138 vector or miR-Con vector. The ratio of Firefly luciferase to Renilla luciferase activity was calculated. The scale bars represent the mean ± S.D. of at least three independent experiments performed in triplicate. ****P < 0.001 vs. pGL6-WT-KSR2+ miR-3138 group. (c) Western blotting analysis of the KSR2 protein expression after various treatments HUVECs underwent miR-Con overexpression, $1 \times 10^{-6}$ mmol/L insulin intervention or miR-3138 overexpression. (d) Western blotting analysis of the KSR2 protein expression after various treatments HUVECs underwent miR-Con overexpression, $1 \times 10^{-6}$ mmol/L insulin intervention or miR-3138 overexpression. The values were measured at three independent experiments in triplicate. The densitometric analysis was performed using ImageJ software and normalizing to actin. The protein expression of KSR2 in NC group was used for normalization control. ****P < 0.001 vs. NC. (e) Under IR condition, the relative mRNA expression of KSR2 after various treatments HUVECs underwent miR-Con inhibition, miR-3138 inhibition + KSR2-Con silencing or miR-3138 inhibition + KSR2 silencing. The mRNA expression of KSR2 was calculated from three independent experiments after normalization with the value in NC group. ****P < 0.001 vs. NC; ####P < 0.001 vs. IR; ^^^^P < 0.001 vs. IR + miR-3138 inhibition + KSR2-Con silencing. (f) Under IR condition, the relative protein expression of KSR2 after various treatments HUVECs underwent miR-Con inhibition, miR-3138 inhibition + KSR2-Con silencing or miR-3138 inhibition + KSR2 silencing. (g) Under IR condition, the relative protein expression of KSR2 after various treatments HUVECs underwent miR-Con inhibition, miR-3138 inhibition + KSR2-Con silencing or miR-3138 inhibition + KSR2 silencing. The values were measured at three independent experiments in triplicate. The densitometric analysis was performed using ImageJ software and normalizing to actin. The protein expression of KSR2 in NC group was used for normalization control. ***P < 0.005 vs. NC; #P < 0.05 vs. IR. ^^^^P < 0.001 vs. IR+miR-3138 inhibition + KSR2-Con silencing.

compared with the IR+miR-3138 inhibition +KSR2-Con silencing group. (Figure 6e, P < 0.001, respectively). Under IR condition, the protein expression of KSR2 was increased to 1.19 times after miR-3138 inhibition compared with the IR group, but reduced significantly after miR-3138 inhibition and KSR2 silencing compared with the IR+miR-3138 inhibition+KSR2-Con silencing group (figure 6f-G, P < 0.05, P < 0.001, respectively). These findings indicated that miR-3138 enhanced the IR of HUVECs by directly targeting KSR2.

## MiR-3138 overexpression could inhibit GLUT4 expression via AMPK pathway

The bioinformatics analysis results showed that miR-3138 may be involved in the AMPK and PI3K/Akt pathways (Figure 3g-h), and it was reported that GLUT4 activity also involved in the two pathways [27–29]. To further validate the correlation of miR-3138, KSR2 and GLUT4 of the two pathways, we explored the effects on the mRNA and protein expressions of GLUT4, AMPK, Akt and PI3K after miR-3138 and KSR2 overexpression and silencing, respectively. In addition, phosphorylation of AMPK (pAMPK), phosphorylation of Akt (pAkt), phosphorylation of PI3K (pPI3K) were measured.

As shown in Figure 7a, the relative mRNA expression of GLUT4 was reduced in IR group and overexpression of miR-3138 further triggered a decrease in the expression of GLUT4 under IR condition (P < 0.001, respectively). The relative mRNA expression of PI3K was reduced in the IR group and further reduced by miR-3138 overexpression under IR condition (Figure 7b, P < 0.005, P < 0.001, respectively). The relative mRNA expression of Akt was also reduced in the IR group and further reduced by miR-3138 overexpression under IR condition (Figure 7c, P < 0.001, respectively). Of note, it has been shown that overexpression of miR-3138 and IR was able to inhibit the ratio of protein expression of pAMPK/AMPK compared with the NC group (Figure 7d-e, P < 0.001 and P < 0.01, respectively). It could be observed that these results indicated that the mRNA expression of GLUT4 possibly involved in the AMPK and PI3K/Akt signaling pathways was

mediated by miR-3138. The miR-Con overexpressi on groups shown in Figure 7a-e were used for suitable control of the experiments.

To provide more evidence about function of regulation GLUT4 by miR-3138, we carried out rescue experiments to observe the protein expression of these molecules. Compared with the NC group, the protein expression of GLUT4 was decreased in IR group (Figure 7f-g, P < 0.001), whereas inhibition of miR-3138 had the opposite effect under IR condition (Figure 7f-g, P < 0.05). Under IR condition, inhibition of KSR2 triggered a decrease in protein expression of GLUT4 compared with the IR+miR-3138 inhibition+KSR2-Con silencing group (Figure 7f-g, P < 0.05).

Consistent with the results shown in Figure 7d-e, the ratio of protein expression of pAMPK/AM PK was decreased in the IR group compared with NC group (Figure 7i-j, P < 0.001). Inhibition of miR-3138 increased the ratio of protein expression of pAMPK/AMPK which was further inhibited when miR-3138 inhibition and KSR2 silencing, under IR condition (Figure 7i-j, P < 0.005, respectively). However, inhibition of miR-3138 increased the ratio of protein expression of pPI3K/PI3K, but KSR2 silencing did not show the inhibition effect of phosphorylation of PI3K (figure 7f, 7h). Similar to the effects of miR-3138 and KSR2 on the ratio of protein expression of pPI3K/PI3K, miR-3138 and KSR2 had no significant influence on phosphorylation of Akt (Figure 7i, 7k). Based on these results, miR-3138 and KSR2 could regulate the expression of GLUT4 and activate the AMPK signaling pathway which has been found to play an important role in IR pathogenesis.

## Discussion

IR is a complex pathological condition resulting from the dysregulation of cellular response to insulin hormone in insulin-dependent cells and is recognized as a pathogenic hallmark and strong risk factor for metabolic syndrome [2,3]. Current studies have proved that a number of factors, such as oxidative stress, inflammation, insulin receptor mutation, ER stress, and mitochondrial dysfunction, contribute to IR which mainly target livers, muscles and adipose tissues [3]. With the growing incidence of diabetic vascular complications,
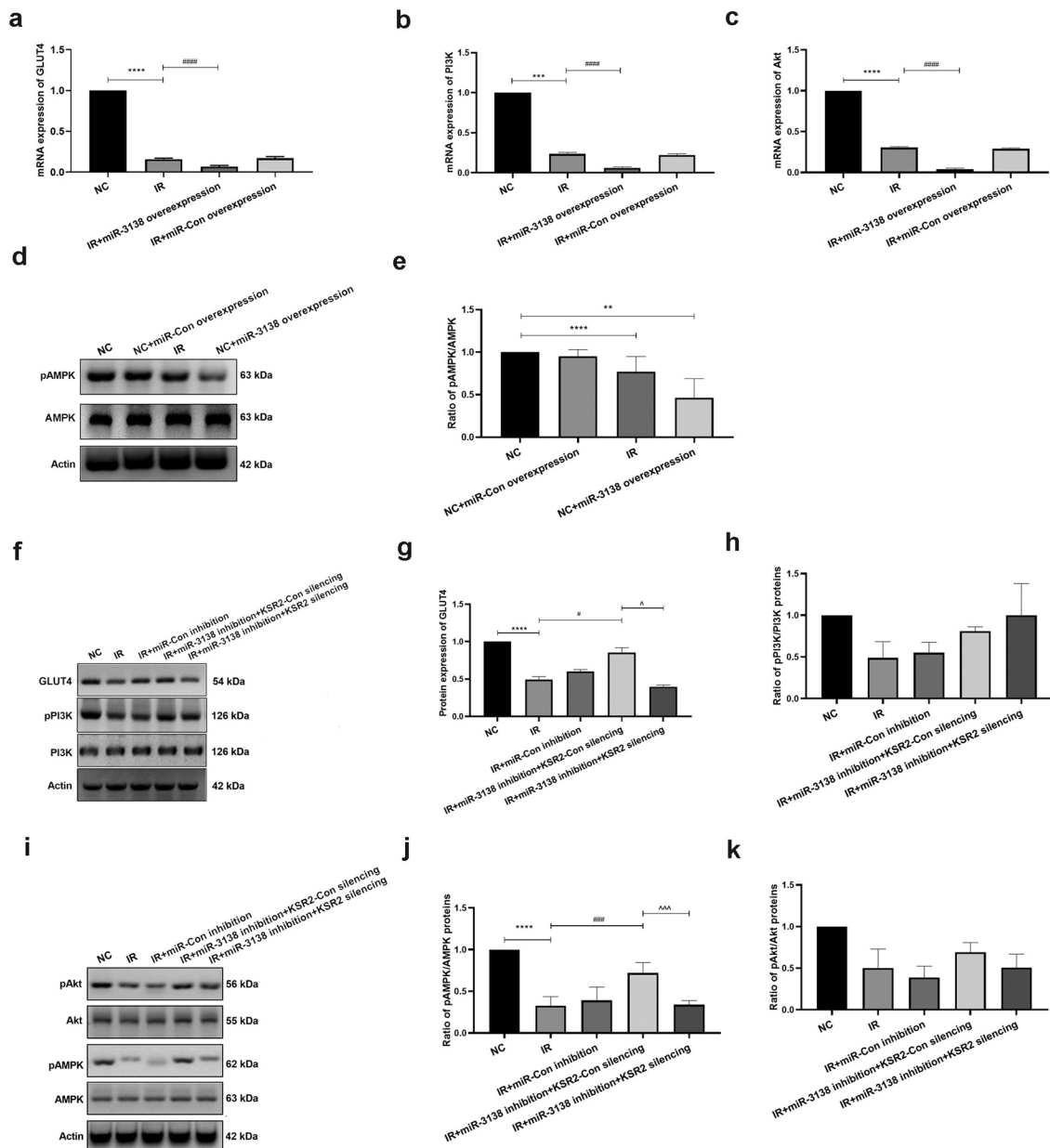
**Figure 7.** The mRNA and protein expression of GLUT4, and molecules in the AMPK and PI3K/Akt pathways of HUVECs after various treatments. (a) Under IR condition, the relative mRNA expression of GLUT4 after treatments HUVECs underwent miR-3138 over-expression or miR-Con overexpression. ****$P < 0.001$ vs. NC; ####$P < 0.001$ vs. IR. (b) Under IR condition, the relative mRNA expression of PI3K after treatments HUVECs underwent miR-3138 overexpression or miR-Con overexpression. ***$P < 0.005$ vs. NC; ####$P < 0.001$ vs. IR. (c) Under IR condition, the relative mRNA expression of Akt after treatments HUVECs underwent miR-3138 overexpression or miR-Con overexpression. ****$P < 0.001$ vs. NC. ####$P < 0.001$ vs. IR. (d) Western blotting analysis of the protein expression of pAMPK and AMPK after various treatments HUVECs underwent miR-Con overexpression, $1 \times 10^{-6}$ mmol/L insulin intervention or miR-3138 overexpression. (e) The ratio of protein expression of pAMPK/AMPK after various treatments HUVECs underwent miR-Con overexpression, $1 \times 10^{-6}$ mmol/L insulin intervention or miR-3138 overexpression. **$P < 0.01$, ****$P < 0.001$ vs. NC. (f) Under IR condition, Western blotting analysis of the protein expression of GLUT4, pPI3K and PI3K after various treatments HUVECs underwent miR-Con inhibition, miR-3138 inhibition + KSR2-Con silencing or miR-3138 inhibition + KSR2 silencing. (g) Under IR condition, the protein expression of GLUT4 after various treatments HUVECs underwent miR-Con inhibition, miR-3138 inhibition + KSR2-Con silencing or miR-3138 inhibition + KSR2 silencing. ****$P < 0.001$ vs. NC; #$P < 0.05$ vs. IR. ^$P < 0.05$ vs. IR+miR-3138 inhibition + KSR2-Con silencing. (h) Under IR condition, the ratio of protein expression of pPI3K/PI3K after various treatments HUVECs underwent miR-Con inhibition, miR-3138 inhibition + KSR2-Con silencing or miR-3138 inhibition + KSR2 silencing. (i) Under IR condition, Western blotting analysis of the protein expression of pAMPK, AMPK, pAkt and Akt after various treatments HUVECs underwent miR-Con inhibition, miR-3138 inhibition + KSR2-Con silencing or miR-3138 inhibition + KSR2 silencing. (j) Under IR condition, the ration of protein expression of pAMPK/AMPK after various treatments HUVECs underwent miR-Con inhibition, miR-3138 inhibition + KSR2-Con silencing or miR-3138 inhibition + KSR2 silencing. ****$P < 0.001$ vs. NC; ###$P < 0.005$ vs. IR. ^^^$P < 0.005$

increasing research attention has been paid to the molecular mechanism of IR in vascular endothelial cells [30]. In this study, we used HUVECs to establish IR cell model for investigating the pathogenesis of IR. Our findings demonstrated that glucose consumption did not decrease with the increase of IR which may be related to the stability of the cell model of IR. Finally, we established an IR cell model induced by $1 \times 10^{-6}$ mmol/L insulin for 48 h.

To date, the molecular mechanism of IR remains unclear [1–3,31]. MiRNAs (short non-coding RNA molecules) regulate the expressions of over 50% of all mammalian genes at the post-transcriptional level [32]. Increasing evidence indicated that miRNAs play crucial roles in IR [17,18]. We performed a miRNA microarray analysis in IR cell model, in which 10 DEMs were found up-regulated or down-regulated. Based on the results of qRT-PCR, the expression level of miR-3138 was highest amongst all (Figure 4a). Furthermore, we found that ROS content was increased and glucose consumption was decreased when miR-3138 overexpression (Figure 5a-c). On the contrary, ROS content was decreased and glucose consumption was increased after miR-3138 inhibition (Figure 5d-e). These results indicated that miR-3138 might improve IR condition resulting in increased ROS content and impaired glucose consumption, which encouraged us to further explore the role of miR-3138 in IR.

Knockout of KSR2 which is a key regulator of glucose homeostasis and energy balance inhibits energy consumption, glucose and lipid metabolism, and then leading to IR [33]. Due to this feature, KSR2 plays an important role in IR pathogenesis. In this study, we found that silencing of KSR2 further triggered a decrease in glucose consumption and enhanced ROS content (Figure 5c-e). Through Targetscan, KSR2 mRNA was predicted as a target of miR-3138 (Figure 6a). Findings from the dual-luciferase reporter assay confirmed that miR-3138 could directly interact with KSR2 (Figure 6b).

Besides, KSR2 was reduced in the IR groups (Figure 6c-g), and further analysis indicated that miR-3138 deteriorates the IR of HUVECs via regulating KSR2 (Figure 5d-e). Thus, we believe that miR-3138 plays a vital role in improving IR condition by directly targeting KSR2.

GLUT4 transports glucose from the extracellular environment into the cells under insulin stimulation [34]. Recent studies showed the sensitive response of GLUT4 to insulin in endothelium cells [20–22]. Recently, GLUT4 has been confirmed to promote insulin-induced translocation in endothelium [23]. Because of miR-3138 and KSR2 contributing to IR accompanied by changes in glucose consumption, we further explored whether miR-3138 and KSR2 affected the expression of GLUT4. MiR-3138 overexpression significantly reduced the expression of GLUT4, but inhibition of miR-3138 markedly increased GLUT4 expression (Figure 7a,7f-g). Moreover, KSR2 silencing triggered a decrease in protein expression of GLUT4 (Figure 7f-g). Our results demonstrated that the expression of GLUT4 was regulated by miR-3138/KSR2 axis. Further investigations focusing on regulation of GLUT4 at the intracellular and cyto-membrane levels are warranted.

There is evidence that AMPK signaling pathway interacts with many molecules including KSR2 and GLUT4 which plays an important role in IR pathogenesis [18,33,35]. AMPK and related phosphorylation can increase glucose transport and glycogen metabolism, and meet the demand of cells for energy [36]. Studies have shown that AMPK and KSR2 can effectively increase the metabolism of carbohydrates and inhibit the effect of cellular IR [31]. And, GLUT4 was also activated by the PI3K/Akt signaling pathway to regulate gene expression and transport [37,38]. It was reported that the AMPK and PI3K/Akt signaling pathways were possibly involved in IR pathogenesis [1,18,33,39,40]. Thus, considering the bioinformatics analysis of our study (figure 3f-h), we

---

vs. IR+miR-3138 inhibition + KSR2-Con silencing. (k) Under IR condition, the ration of protein expression of pAkt/Akt after various treatments HUVECs underwent miR-Con inhibition, miR-3138 inhibition + KSR2-Con silencing or miR-3138 inhibition + KSR2 silencing. The mRNA expressions of GLUT4, PI3K and Akt were calculated from three independent experiments after normalization with the value in NC group. The protein expressions of GLUT4, pAMPK, AMPK, pPI3K, PI3K, pAkt, Akt and Actin were calculated from three independent experiments and normalizing to NC group after normalization with the Actin. The densitometric analysis was performed using ImageJ software in Western Blotting.
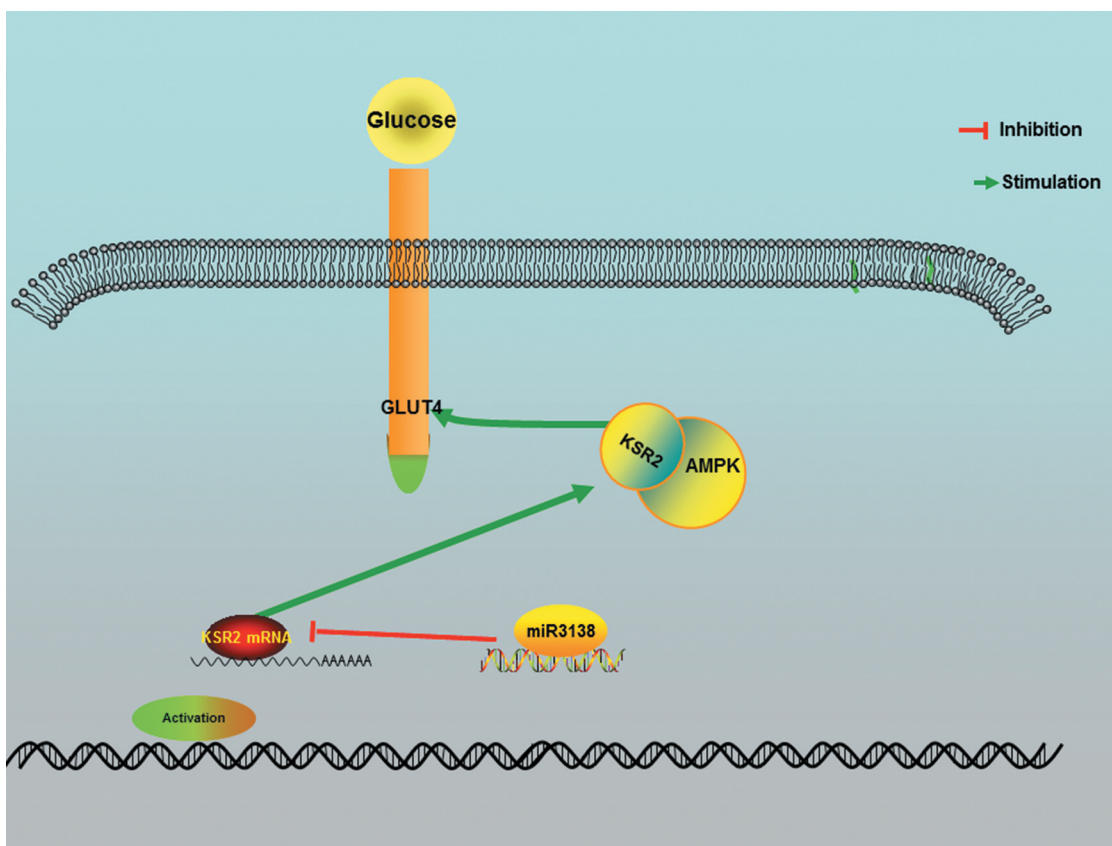
**Figure 8.** MiR-3138 deteriorates IR through the KSR2/AMPK/GLUT4 signaling pathway.

further investigated the expression of AMPK and PI3K/Akt after miR-3138 and KSR2 overexpression and inhibition in IR cell model.

Our results showed that the phosphorylation of AMPK was decreased in IR groups and miR-3138 overexpression (Figure 7d-e). Moreover, under the IR condition, the phosphorylation of AMPK was increased after miR-3138 inhibition, but decreased after KSR2 silencing (Figure 7i-j). In addition, we further explored whether miR-3138 affected KSR2 through the PI3K/Akt signaling. And it was a pity that KSR2 silencing did not show the inhibition effect of phosphorylation of PI3K. Further, there was no statistical significance in the rescue experiment about PI3K/Akt signaling (Figure 7f, 7h-i, 7k). Our results indicated that miR-3138 by interacting with KSR2 could inhibit the GLUT4/AMPK signaling pathway rather than the PI3K/Akt signaling pathway (Figure 8).

In conclusion, our findings suggest that miR-3138 deteriorates IR via KSR2/AMPK/GLUT4 signaling pathway. These results could serve as the starting point to elucidate the molecular mechanism of the pathogenesis of IR, and miR-3138 and KSR2 could be identified as novel targets for IR prevention.

## Disclosure of interest

The authors declare no conflicts of interest.

## Disclosure statement

No potential conflict of interest was reported by the authors.

## Funding

## References

[1] Petersen MC, Shulman GI. Mechanisms of insulin action and insulin resistance. Physiol Rev. 2018;98 (4):2133–2223.

[2] Yaribeygi H, Farrokhi FR, Butler AE, et al. Insulin resistance: review of the underlying molecular mechanisms. J Cell Physiol. 2019;234(6):8152–8161.

[3] Freeman AM, Pennings N. Insulin resistance. In: StatPearls.. Treasure Island (FL); 2019; 1–22

[4] Hojlund K. Metabolism and insulin signaling in common metabolic disorders and inherited insulin resistance. Dan Med J. 2014;61(7):B4890.

[5] Katsoulieris EN, Drossopoulou GI, Kotsopoulou ES, et al. High glucose impairs insulin signaling in the glomerulus: an in vitro and ex vivo approach. PLoS One. 2016;11(7):e0158873.

[6] Di Meo S, Iossa S, Venditti P. Skeletal muscle insulin resistance: role of mitochondria and other ROS sources. J Endocrinol. 2017;233(1):R15–r42.

[7] Bhattacharjee CK, Paine SK, Mahanta J, et al. Expression of inflammasome complex mRNA and its targeted microRNA in type 2 diabetes mellitus: A possible predictor of the severity of diabetic nephropathy. J Diabetes. 2019;11(1):90–92

[8] Parvin M, Jahan PK, Sarkar ZH, et al. *Correction to: functional polymorphism located in the microRNA binding site of the insulin receptor (INSR) gene confers risk for type 2 diabetes mellitus in the bangladeshi population.* Biochem Genet. 2018; DOI:10.1007/s10528-018-9872-7

[9] Strutz J, Cvitic S, Hackl H, et al. Gestational diabetes alters microRNA signatures in human feto-placental endothelial cells depending on fetal sex. Clin Sci (Lond). 2018;132(22):2437–2449.

[10] Torella D, Laconetti C, Tarallo R, et al. MicroRNA regulation of the hyper-proliferative phenotype of vascular smooth muscle cells in diabetes mellitus. Diabetes. 2018;67(12):2554–2568.

[11] Vaishya S, Sarwade RD, Seshadri V. MicroRNA, proteins, and metabolites as novel biomarkers for prediabetes, diabetes, and related complications. Front Endocrinol (Lausanne). 2018;9:180.

[12] Wang P, Wang H, Li C, et al. Dysregulation of microRNA-657 influences inflammatory response via targeting interleukin-37 in gestational diabetes mellitus. J Cell Physiol. 2018;234(5):7141–7148

[13] Greenhill C. Genetics: KSR2 mutations affect energy balance, insulin sensitivity and cellular fuel oxidation. Nat Rev Endocrinol. 2014;10(1):1.

[14] Pearce LR, Atanassova N, Banton M, et al. KSR2 mutations are associated with obesity, insulin resistance, and impaired cellular fuel oxidation. Cell. 2013;155(4):765–777.

[15] Revelli JP, Smith D, Allen J, et al. Profound obesity secondary to hyperphagia in mice lacking kinase suppressor of ras 2. Obesity (Silver Spring). 2011;19(5):1010–1018.

[16] Wang Y, Ma T, Zhu YS, et al. The KSR2-rs7973260 polymorphism is associated with metabolic phenotypes, but not psychological phenotypes, in chinese elders. Genet Test Mol Biomarkers. 2017;21(7):416–421.

[17] Tekola-Ayele F, Doumatey AP, Shriner D, et al. Genome-wide association study identifies African-ancestry specific variants for metabolic syndrome. Mol Genet Metab. 2015;116(4):305–313.

[18] Fernandez MR, Henry MD, Lewis RE. Kinase suppressor of Ras 2 (KSR2) regulates tumor cell transformation via AMPK. Mol Cell Biol. 2012;32(18):3718–3731.

[19] Govers R. Molecular mechanisms of GLUT4 regulation in adipocytes. Diabetes Metab. 2014;40(6):400–410.

[20] Pillion DJ, Haskell JF, Meezan E. Cerebral cortical microvessels: an insulin-sensitive tissue. Biochem Biophys Res Commun. 1982;104(2):686–692.

[21] King GL, Goodman AD, Buzney S, et al. Receptors and growth-promoting effects of insulin and insulinlike growth factors on cells from bovine retinal capillaries and aorta. J Clin Invest. 1985;75(3):1028–1036.

[22] Atkins KB, Seki Y, Saha J, et al. Maintenance of GLUT4 expression in smooth muscle prevents hypertension-induced changes in vascular reactivity. Physiol Rep. 2015;3(2):e12299.

[23] Vilaro S, Palacín M, Pilch PF, et al. Expression of an insulin-regulatable glucose carrier in muscle and fat endothelial cells. Nature. 1989;342(6251):798–800.

[24] D'Souza K, Kane DA, Touaibia M, et al. Autotaxin is regulated by glucose and insulin in adipocytes. Endocrinology. 2017;158(4):791–803.

[25] Lo KA, Labadorf A, Kennedy N, et al. Analysis of in vitro insulin-resistance models and their physiological relevance to in vivo diet-induced adipose insulin resistance. Cell Rep. 2013;5(1):259–270.

[26] Eruslanov E, Kusmartsev S. Identification of ROS using oxidized DCFDA and flow-cytometry. Methods Mol Biol. 2010;594:57–72.

[27] Vlavcheski F, Baron D, Vlachogiannis IA, et al. Carnosol increases skeletal muscle cell glucose uptake via AMPK-dependent GLUT4 glucose transporter translocation. Int J Mol Sci. 2018;19(5):1321–1351

[28] Xiong H, Zhang S, Zhao Z, et al. Antidiabetic activities of entagenic acid in type 2 diabetic db/db mice and L6 myotubes via AMPK/GLUT4 pathway. J Ethnopharmacol. 2018;211:366–374.

[29] Wang Y, Wen L, Zhou S, et al. Effects of four weeks intermittent hypoxia intervention on glucose homeostasis, insulin sensitivity, GLUT4 translocation, insulin receptor phosphorylation, and Akt activity in skeletal muscle of obese mice with type 2 diabetes. PLoS One. 2018;13(9):e0203551.

[30] Kong Y, Gao Y, Lan D, et al. Trans-repression of NFkappaB pathway mediated by PPARgamma improves vascular endothelium insulin resistance. J Cell Mol Med. 2019;23(1):216–226.

[31] Manna P, Achari AE, Jain SK. 1,25(OH)2-vitamin D3 upregulates glucose uptake mediated by SIRT1/IRS1/

GLUT4 signaling cascade in C2C12 myotubes. Mol Cell Biochem. 2018;444(1–2):103–108.

[32] Aledo JC, Lavoie L, Volchuk A, et al. Identification and characterization of two distinct intracellular GLUT4 pools in rat skeletal muscle: evidence for an endosomal and an insulin-sensitive GLUT4 compartment. Biochem J. 1997;325 ((Pt 3)):791–803.

[33] Costanzo-Garvey DL, Pfluger PT, Dougherty MK, et al. KSR2 is an essential regulator of AMP kinase, energy expenditure, and insulin sensitivity. Cell Metab. 2009; 10(5):366–378.

[34] Govers R. Cellular regulation of glucose uptake by glucose transporter GLUT4. Adv Clin Chem. 2014;66:173–240.

[35] Guo L, Costanzo-Garvey DL, Smith DR, et al. Kinase suppressor of Ras 2 (KSR2) expression in the brain regulates energy balance and glucose homeostasis. Mol Metab. 2017;6(2):194–205.

[36] Saha AK, Ruderman NB. Malonyl-CoA and AMP-activated protein kinase: an expanding partnership. Mol Cell Biochem. 2003;253(1–2):65–70.

[37] Zhao P, Ming Q, Qiu J, et al. Ethanolic extract of folium sennae mediates the glucose uptake of L6 cells by GLUT4 and Ca(2). Molecules. 2018;23 (11):2934–2972

[38] Yang Z, Wu F, He Y, et al. A novel PTP1B inhibitor extracted from ganoderma lucidum ameliorates insulin resistance by regulating IRS1-GLUT4 cascades in the insulin signaling pathway. Food Funct. 2018;9(1):397–406.

[39] Manna P, Achari AE, Jain SK. Vitamin D supplementation inhibits oxidative stress and upregulate SIRT1/AMPK/GLUT4 cascade in high glucose-treated 3T3L1 adipocytes and in adipose tissue of high fat diet-fed diabetic mice. Arch Biochem Biophys. 2017;615:22–34.

[40] Wan CP, Wei YG, Li XX, et al. Piperine regulates glucose metabolism disorder in HepG2 cells of insulin resistance models via targeting upstream target of AMPK signaling pathway. Zhongguo Zhong Yao Za Zhi. 2017;42(3):542–547.